Validation of semi-automatic segmentation of the left atrium

ARTICLE *in* PROCEEDINGS OF SPIE - THE INTERNATIONAL SOCIETY FOR OPTICAL ENGINEERING · MARCH 2008

Impact Factor: 0.2 · DOI: 10.1117/12.773097

Validation of semi-automatic segmentation of the left atrium

M.E. Rettmann[a], D.R. Holmes III[a], J.J. Camp[a], D.L. Packer[b], and R.A. Robb[a]

[a]Biomedical Imaging Resource;
[b]Division of Cardiology/Electrophysiology
Mayo Clinic College of Medicine, Rochester, MN, USA

ABSTRACT

Catheter ablation therapy has become increasingly popular for the treatment of left atrial fibrillation. The effect of this treatment on left atrial morphology, however, has not yet been completely quantified. Initial studies have indicated a decrease in left atrial size with a concomitant decrease in pulmonary vein diameter. In order to effectively study if catheter based therapies affect left atrial geometry, robust segmentations with minimal user interaction are required. In this work, we validate a method to semi-automatically segment the left atrium from computed-tomography scans. The first step of the technique utilizes seeded region growing to extract the entire blood pool including the four chambers of the heart, the pulmonary veins, aorta, superior vena cava, inferior vena cava, and other surrounding structures. Next, the left atrium and pulmonary veins are separated from the rest of the blood pool using an algorithm that searches for thin connections between user defined points in the volumetric data or on a surface rendering. Finally, pulmonary veins are separated from the left atrium using a three dimensional tracing tool. A single user segmented three datasets three times using both the semi-automatic technique as well as manual tracing. The user interaction time for the semi-automatic technique was approximately forty-five minutes per dataset and the manual tracing required between four and eight hours per dataset depending on the number of slices. A truth model was generated using a simple voting scheme on the repeated manual segmentations. A second user segmented each of the nine datasets using the semi-automatic technique only. Several metrics were computed to assess the agreement between the semi-automatic technique and the truth model including percent differences in left atrial volume, DICE overlap, and mean distance between the boundaries of the segmented left atria. Overall, the semi-automatic approach was demonstrated to be repeatable within and between raters, and accurate when compared to the truth model. Finally, we generated a visualization to assess the spatial variability in the segmentation errors between the semi-automatic approach and the truth model. The visualization demonstrates the highest errors occur at the boundaries between the left atium and pulmonary veins as well as the left atrium and left atrial appendage. In conclusion, we describe a semi-automatic approach for left atrial segmentation that demonstrates repeatability and accuracy, with the advantage of significant time reduction in user interaction time.

Keywords: Left Atrial Segmentation, Image-Guided Ablation, Left Atrial Fibrillation, Left Atrium

1. INTRODUCTION

Catheter ablation therapy has become increasingly popular for the treatment of left atrial fibrillation. The effect of this treatment on left atrial morphology, however, has not yet been completely quantified. Initial studies have indicated a decrease in left atrial volume[1,2] along with a decrease in pulmonary vein size.[1–3] In order to effectively assess the affect of catheter-based therapies on left atrial geometry, robust segmentations with minimal user interaction are required. As opposed to segmentation methodologies for the left ventricle, relatively few algorithms have been reported that specifically target left atrial segmentation. One previously described approach employs a region growing approach to extract the entire blood pool, followed by detection of appropriate cuts using geometric properties.[4] Another method[5] utilizes a shape model for left atrial segmentation. Of these techniques, our proposed methodology is more similar in spirit to that of,[4] in that we start with the entire blood pool extracted from seeded region growing, followed by separation into the component anatomical structures (left atrium, pulmonary veins, and left atrial appendage). The results from the semi-automatic method are assessed based on inter and intra-rater repeatability, as well as comparison with a manually generated truth model.

Further author information: (Send correspondence to M.E.R.)
M.E.R.: E-mail: rettmann.maryam@mayo.edu

Medical Imaging 2008: Physiology, Function, and Structure from Medical Images
edited by Xiaoping P. Hu, Anne V. Clough, Proc. of SPIE Vol. 6916, 691625, (2008)
1605-7422/08/$18 · doi: 10.1117/12.773097

2. METHODS

The steps of the semi-automatic method are illustrated in Figure 1 and described as follows. First, seeded region growing is used to extract the blood pool using a tool in which the user can interactively adjust the threshold (Figure 1(a)). This step extracts the entire blood pool including the four chambers of the heart, the pulmonary veins, aorta, superior vena cava, inferior vena cava and other surrounding structures (Figure 1(b)). The next step is to separate the left atrium and pulmonary veins from surrounding cardiac structures. This is accomplished using an algorithm that searches for thin connections between points defined by the user either in the volumetric data or on a surface rendering. This step is iteratively repeated until only the left atrium and pulmonary veins remain. The result of the first iteration is shown in Figure 1(c). Figure 1(d) shows seedpoints used for the next iteration with the result in Figure 1(e). A 3D tracing tool was used to remove sections of the pulmonary veins beyond the first branching point as well as to separate the pulmonary veins and left atrial appendage from the left atrium. The final result is shown in Figure 2(a) (front view) and Figure 2(b) (back view).

Manual tracing of the left atrium was done using the Analyze[6] software. The boundary between the left atrium and each pulmonary vein was defined as the line that connects the points of maximal curvature on each side of the pulmonary vein. The same rule was used for the boundary with the left atrial appendage. The mitral valve was not included as part of the left atrium.

Three datasets were duplicated three times and randomized. A single user segmented each of the nine datasets using both the semi-automatic technique as well as manual tracing. Figure 3 illustrates both the manually traced and semi-automatic segmentation of the same dataset. The comparison is shown as a volume rendering, however, the manual tracing was done image by image on axial cross-sections. Visual inspection indicates overall agreement between the two segmentations. Visualization of the manual segmentation in 3D demonstrates the challenge of separating the pulmonary veins and left atrial appendage from the left atrium on image cross-sections. The boundary is somewhat jagged as compared with the semi-automatic segmentation. Delineation of this boundary using the semi-automatic segmentation is done using a volumetric rendering, thereby making it easier to create a smooth boundary in three-dimensions. A second user segmented each of the nine datasets using the semi-automatic technique only. The user interaction time for the semi-automatic technique was approximately forty-five minutes per dataset and the manual tracing required four to eight hours depending on the resolution and number of slices in the dataset.

A truth model was generated for each of the subjects using the set of three manual tracings as follows. First, one segmentation is chosen as the reference dataset and the additional two segementations are registered to the reference segmentation. A single truth model for each subject is created using a simple voting scheme. At each voxel, foreground or background is assigned based on a majority vote from the three segmentations.

Several metrics were computed to assess the agreement between the semi-automatic technique and the truth model. The first metric is the percentage difference between the left atrial volumes, defined as $((vol(T) - vol(S))/vol(T)) * 100$ where $vol(T)$ is the volume from the truth model and $vol(S)$ is the volume from the semi-automatic segmentation. The second metric is the Dice overlap,[7] defined as $2(T \cap S)/(T + S)$ where T is the manual segmentation and S is the semi-automatic segmentation. A third metric is the distance from the boundary of the semi-automatic segmentation to the boundary of the truth model. To compute this metric, a distance transform is computed from the boundary of the truth model. Next, a mask volume containing only the boundary of the semi-automatic segmentation is constructed. The mask volume is multiplied by the distance transform volume to obtain boundary distance measures. The mean and standard deviation of these distance measures are computed for each semi-automatic segmentation. Finally, in order to assess the spatial distribution of the border errors, these errors are mapped onto the left atrial surface and visualized.

3. RESULTS

The repeatability of the manual segmentations, assessed as percent differences in left atrial volume, is reported in Table 1. Manual segmentations were done on each subject three separate times. The various segmentation pairs are given across the top of the table. The overall repeatability is 3.31%, and the repeatability in 7 of the 9 image pairs was less than 5%. The within-rater repeatability of the semi-automatic segmentations, assessed as percent differences in left atrial volume, is reported in Table 2. The mean repeatability for rater 1 is 4.89%, and the

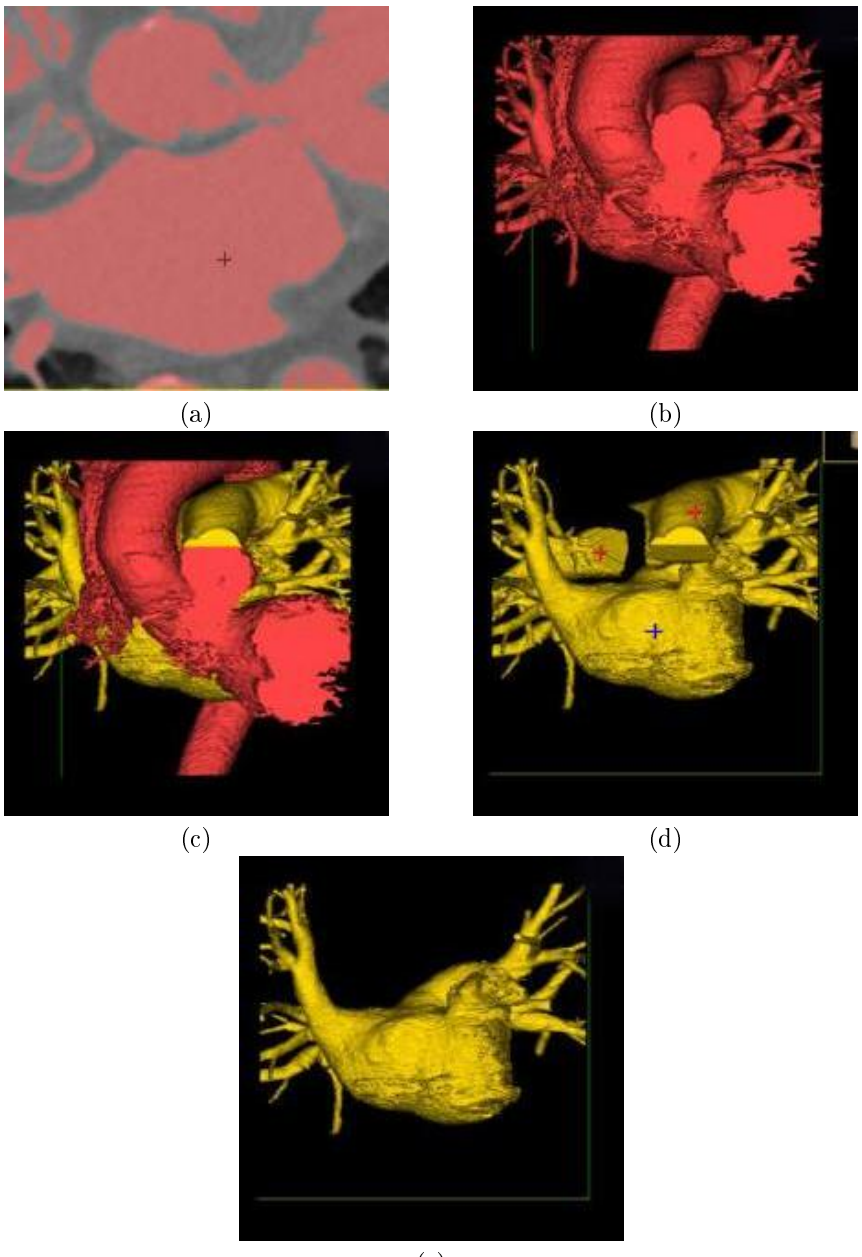

Figure 1. Steps in semi-automatic segmentation technique. (a) Seeded region growing. (b) Volume rendered result of seeded region growing. (c) Result of initial region separation (red indicates one region, yellow indicates second region). (d) Seedpoints selected for second separation. (e) Isolated left atrium and pulmonary veins. (Color images appear on CD-ROM).

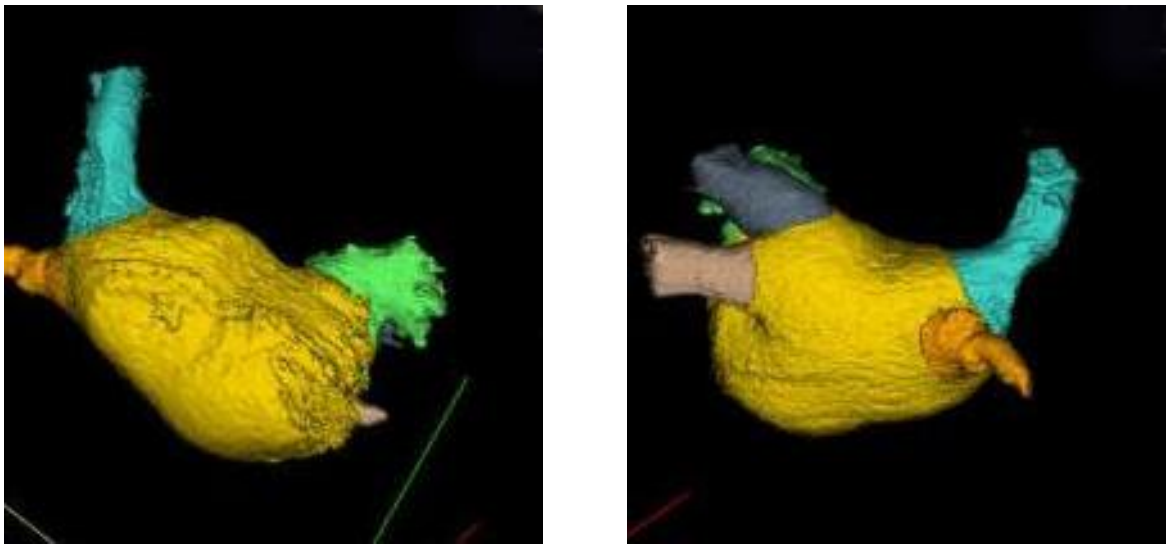

(a) (b)

Figure 2. (a) Front view of semi-automatic segmentation. (b) Back view of semi-automatic segmentation. (Color images appear on CD-ROM).

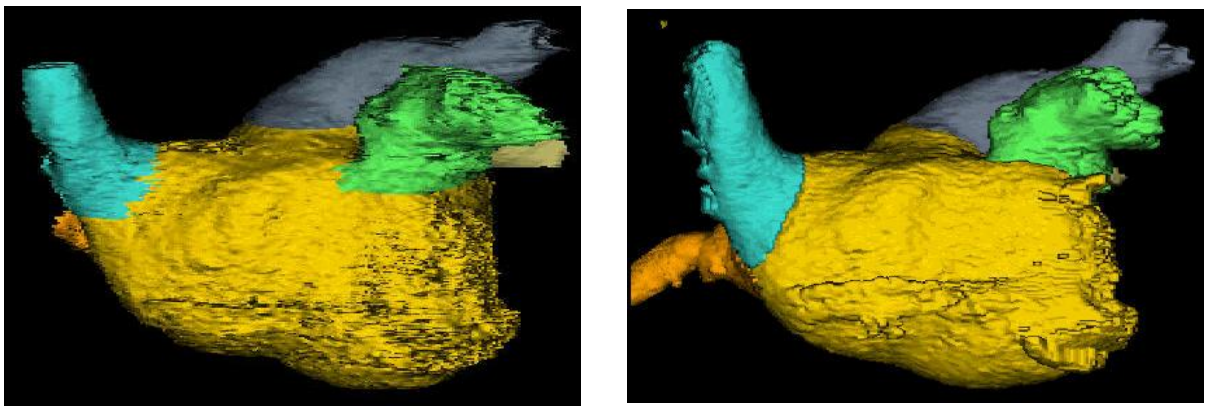

(a) (b)

Figure 3. (a) Manually traced and (b) semi-automatic segmentation of the same dataset. (Color images appear on CD-ROM).

	1&2	2&3	1&3	Mean
Subject 1	2.08	5.69	3.73	3.83
Subject 2	1.96	3.07	1.05	2.03
Subject 3	4.08	2.08	6.07	4.08
Overall Mean				3.31

Table 1. Repeatability for manual segmentations, quantified as percent differences in left atrial volume. 1&2=Differences in segmentations 1 and 2, 2&3=Differences in segmentations 2 and 3, 1&3=Differences in segmentations 1 and 3.

	R1 1&2	R1 2&3	R1 1&3	Mean	R2 1&2	R2 2&3	R2 1&3	Mean
Subject 1	7.21	5.72	1.91	4.95	6.52	10.36	4.52	7.13
Subject 2	5.50	0.89	4.39	6.76	13.21	9.07	5.34	9.21
Subject 3	4.45	8.20	3.38	5.34	2.84	2.63	0.28	1.92
Overall Mean				4.89				6.08

Table 2. Intra-rater repeatability for semi-automatic segmentation, quantified as percent differences in left atrial volume. R1=rater 1, R2=rater 2. 1&2=Differences in segmentations 1 and 2, 2&3=Differences in segmentations 2 and 3, 1&3=Differences in segmentations 1 and 3.

mean repeatability for rater 2 is 6.08%. The between-rater repeatability for the semi-automated segmentations is reported in Table 3. The mean inter-rater repeatability is 5.57% which is similar in magnitude to the intra-rater repeatability.

Accuracy (as opposed to repeatability) of the semi-automatic segmentation methodology is quantified using several metrics. The first is percent difference in left atrial volume between the semi-automatic approach and the truth model, as reported in Table 4. The mean accuracy for rater 1 is 2.98% and the mean accuracy for rater 2 is 3.24%. The second metric for quantifying accuracy is the DICE overlap between each semi-automatic segmentation and the truth model, as reported in Table 5. The mean DICE overlap for rater 1 is 0.97 and the mean DICE overlap for rater 2 is 0.92. The final metric for assessing accuracy is the distance from the boundary of the truth model to the boundary of each semi-automatic segmentation as reported in Table 6. The mean distances range from 0.24 mm to 3.94 mm. Finally, in order to assess the spatial distribution of the border errors, these errors were mapped onto the left atrial surface and visualized, as illustrated in Figure 4. This figure demonstrates that the largest errors occur at the boundary of the left atrium and pulmonary veins, as well as the boundary between the left atrium and left atrial appendage.

4. CONCLUSIONS AND DISCUSSION

In this work, we describe a semi-automatic technique for segmenting the left atrium from CT datasets. The semi-automatic methodology provides a 5 to 10 times improvement in user interaction time as compared with manual tracing on image cross-sections. In addition, since boundaries are delineated on a 3D rendering, more natural separations can be defined between the left atrium and pulmonary veins as well as the left atrium and left atrial appendage. Overall, the semi-automatic approach was demonstrated to be repeatable within and between raters, and accurate when compared to the truth model. Mean distances between the truth model and semi-automatic segmentations were, in general, relatively small, ranging in magnitude from 0.24 mm to 3.94 mm. A surface visualization of the errors indicates the highest errors occur at the junction between the left

	1&2	2&3	1&3	Mean
Subject 1	5.06	8.99	7.59	7.21
Subject 2	6.64	13.32	0.05	6.67
Subject 3	2.22	0.57	5.69	2.83
Overall Mean				5.57

Table 3. Inter-rater repeatability for semi-automatic segmentations, quantified as percent differences in left atrial volume. 1&2=Differences in segmentations 1 and 2, 2&3=Differences in segmentations 2 and 3, 1&3=Differences in segmentations 1 and 3.

	R1 Seg1	R1 Seg2	R1 Seg3	Mean	R2 Seg1	R2 Seg2	R2 Seg3	Mean
Subject 1	4.36	3.17	2.37	3.30	0.92	5.54	5.40	3.95
Subject 2	0.89	5.81	0.01	2.24	5.69	8.28	0.04	4.67
Subject 3	2.21	2.34	5.67	3.41	0.06	2.90	0.34	1.10
Overall Mean				2.98				3.24

Table 4. Accuracy for semi-automatic segmentation as compared to truth model, quantified using percent differences in left atrial volume. R1=rater 1, R2=rater 2, Seg1=Segmentation 1, Seg2=Segmentation 2, Seg3=Segmentation 3.

	R1 Seg1	R1 Seg2	R1 Seg3	Mean	R2 Seg1	R2 Seg2	R2 Seg3	Mean
Subject 1	0.94	0.97	0.96	0.96	0.90	0.89	0.90	0.90
Subject 2	0.98	0.97	0.98	0.98	0.94	0.93	0.93	0.93
Subject 3	0.97	0.97	0.98	0.97	0.93	0.94	0.93	0.93
Overall Mean				0.97				0.92

Table 5. Accuracy of semi-automatic segmentation as compared to truth model, quantified using DICE overlap. R1=rater 1, R2=rater 2, Seg1=Segmentation 1, Seg2=Segmentation 2, Seg3=Segmentation 3.

	R1 Seg1	R1 Seg2	R1 Seg3	R2 Seg1	R2 Seg2	R2 Seg3
Subject 1	2.04 (5.95)	0.52 (0.96)	0.50 (1.00)	3.28 (5.40)	3.93 (8.22)	3.94 (5.40)
Subject 2	2.96 (10.64)	3.27 (4.98)	0.24 (0.43)	1.28 (3.26)	3.47 (4.57)	1.30 (2.35)
Subject 3	1.35 (5.27)	0.52 (1.61)	0.25 (0.57)	1.33 (2.26)	1.26 (2.39)	1.11 (1.87)

Table 6. Mean (std) in mm of error on border of left atrial segmentation. R1=rater 1, R2=rater 2, Seg1=Segmentation 1, Seg2=Segmentation 2, Seg3=Segmentation 3.

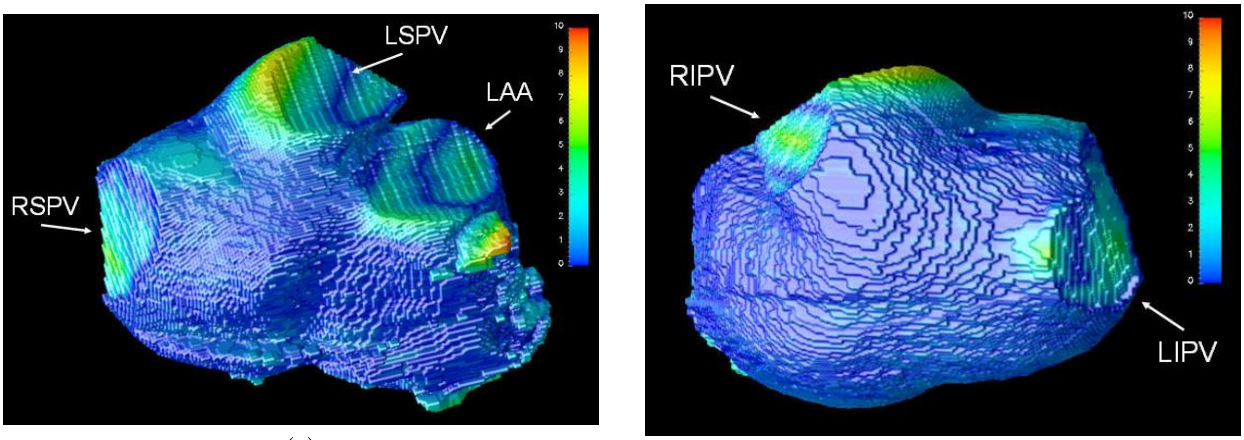

(a) (b)

Figure 4. Distance errors (in mm) displayed on the left atrium from (a) front view and (b) back view. The locations where the pulumonary veins and left atrial appendage attach are indicated with labels and arrows. LAA=left atrial appendage, LSPV=left superior pulmonary vein, LIPV=left inferior pulmonary vein, RSPV=right superior pulmonary vein, RIPV=right inferior pulmonary vein. (Color images appear on CD-ROM).

atrium and pulmonary veins as well as the left atrium and left atrial appendage. As demonstrated in Figure 3, however, it is not clear that the manual delineation of the junction between the left atrium and pulmonary veins is truly more accurate. The challenge in manual tracing on image cross-sections is that the full three dimensional information is not available, therefore, it can be difficult to properly define borders that are oblique to the image plane. One can conclude, however, that in order to obtain high quality segmentations of the left atrium, this junction is extremely important to define in a repeatable, robust fashion. We are currently pursuing a technique to automatically identify the ostia of the pulmonary veins in a quantitative fashion using the full three-dimensional information of the connection between the pulmonary veins and left atrium. Once located, the ostium can be used as the point to define a cutting plane between these structures. In conclusion, this work demonstrates a validated, semi-automatic technique for left atrial segementions with several advantages over manual tracing. In-depth analysis of the results underscores the importance of robustly defining boundaries between the left atrium and its associated structures.

ACKNOWLEDGMENTS

The authors thank Cindy Ge for assistance with left atrial segmentations. This work was partially supported by NIH/NIBIB grant #EB91959028.

REFERENCES

1. K. Lemola, M. Sneider, B. Desjardins, I. Case, A. Chugh, B. Hall, P. Cheung, E. Good, J. Han, K. Tamirisa, F. Bogun, F. Pelosi Jr., E. Kazerooni, F. Morady, and H. Oral, "Effects of left atrial ablation of atrial fibrillation on size of the left atrium and pulmonary veins.," *Heart Rhythm* **1**(5), pp. 576–581, 2004.
2. H. Tsao, M. Wu, B. Huang, S. Lee, K. Lee, C. Tai, Y. Lin, M. Hsieh, J. Kuo, M. Lei, and S. Chen, "Morphologic remodeling of pulmonary veins and left atrium after catheter ablation of atrial fibrillation.," *J. Cardiovasc Electrophysiol* **16**, pp. 7–12, 2005.
3. C. Scharf, M. Sneider, I. Case, A. Chugh, S. Lai, F. Pelosi Jr., B. Knight, E. Kazerooni, F. Morady, and H. Oral, "Anatomy of the pulmonary veins in patients with atrial fibrillation and effects of segmental ostial ablation analyzed by computed tomography.," *J Cardiovasc Electrophysiol* **14**, pp. 150–155, 2003.
4. M. John and N. Rahn, "Automatic left atrium segmentation by cutting the blood pool at narrowings," in *Medical Image Computing and Computer Assisted Intervention (MICCAI)*, **3750**, pp. 798–805, 2005.
5. J. Berg and C. Lorenz, "Accurate left atrium segmentation in multislice CT images using a shape model.," in *Proc. SPIE Medical Imaging*, 2005.
6. R. A. Robb and D. P. Hanson, "Analyze: A software system for biomedical image analysis," in *First Conference on Visualization in Biomedical Computing*, **1**, pp. 507–518, 1990.
7. L. Dice, "Measures of the amount of ecologic association between species," *Ecology* **26**, pp. 297–302, 1945.